

Resource Scheduling Under Uncertainty in a Smart Grid with Renewables and Plug-in Vehicles

Ahmed Yousuf Saber, *Senior Member, IEEE*, and Ganesh Kumar Venayagamoorthy, *Senior Member, IEEE*

Abstract—The power system and transportation sector are our planet’s main sources of greenhouse gas emissions. Renewable energy sources (RESs), mainly wind and solar, can reduce emissions from the electric energy sector; however, they are very intermittent. Likewise, next generation plug-in vehicles, which include plug-in hybrid electric vehicles and electric vehicles with vehicle-to-grid capability, referred to as gridable vehicles (GVs) by the authors, can reduce emissions from the transportation sector. GV’s can be used as loads, energy sources (small portable power plants) and energy storage units in a smart grid integrated with renewable energy sources. However, uncertainty surrounds the controllability of GV’s. Forecasted load is used in unit commitment (UC); however, the actual load usually differs from the forecasted one. Thus, UC with plug-in vehicles under uncertainty in a smart grid is very complex considering smart charging and discharging to and from various energy sources and loads to reduce both cost and emissions. A set of valid scenarios is considered for the uncertainties of wind and solar energy sources, load and GV’s. In this paper, an optimization algorithm is used to minimize the expected cost and emissions of the UC schedule for the set of scenarios. Results are presented indicating that the smart grid has the potential to maximally utilize RESs and GV’s to reduce cost and emissions from the power system and transportation sector.

Index Terms—Cost, emissions, plug-in electric vehicles, renewable energy, scenario, smart grid, uncertainty, unit commitment.

NOMENCLATURE

δ_D, δ_W	Sets of discrete distributions of load, wind power, solar power, and vehicles, respectively.
$\delta_{PV}, \delta_{V2G}$	
$\mu(t)$	Solar insolation at time t .
Ψ_{pre}/Ψ_{dep}	Present/departure state of charge.
Ψ_{min}/Ψ_{max}	Min./max. state of charge.
ξ	Efficiency (battery).
$\mathcal{F}C()$	Fuel cost function.
$\mathcal{S}C_i()$	Start-up cost function of unit i .
$\mathcal{E}C_i()$	Emission cost function of unit i .
A	Area.
$c-cost_i$	Cold start cost of i th unit.
$D(t)$	Load demand at time t .
$E(.)$	Expectation.

$h-cost_i$	Hot start cost of i th unit.
H	Scheduling hours.
Ite	Current iteration.
$I_i(t)$	Status of unit i at hour t (1/0 for on/off).
$MaxIte$	Maximum iteration.
N	Number of units.
$N_{V2G}(t)$	No. of vehicles connected to the grid at hour t .
N_{V2G}^{max}	Total vehicles in the system.
N_{GV}	Number of GV’s.
$P_i^s(t)$	Power of unit i at time t considering scenario s .
$P_{wind}^s(t)$	Power from wind farm at time t considering scenario s .
$P_{solar}^s(t)$	Power from solar farm at time t considering scenario s .
P_i^{max}/P_i^{min}	Max./min. output limit of i th unit.
P_{v_j}	Capacity of vehicle j .
$P_{v_j}(t)$	Charge of vehicle j at time t .
$rand$	A random number between 0 and 1.
$R(t)$	System reserve requirement at hour t .
S	Set of scenarios.
$U(1)$	A uniform number between 0 and 1.
$V2G/G2V$	Vehicle-to-grid/grid-to-vehicle.

I. INTRODUCTION

WITH INCREASING concern over global climate change, policy makers are promoting renewable energy sources (RESs) as a means of meeting emissions reduction targets. The alarming rate at which global energy reserves are depleting is a major worldwide concern at economic, environmental, industrial, and community levels [1]–[3]. A partial solution to this crisis is: 1) the use of decentralized renewable energy; and 2) the application of next-generation plug-in vehicles, which include plug-in hybrid electric vehicles (PHEVs) and electric vehicles (EVs) with vehicle-to-grid (V2G) capability, renamed “gridable vehicles” (GVs) by the authors. A technical report from the National Renewable Energy Laboratory (NREL) has reported significant reductions in net CO₂ emissions from PHEVs [4]. Considering cost advantages, a study by the Electric Power Research Institute, Palo Alto, CA, found a significant potential market for PHEVs [5].

PHEV and EV researchers have mainly concentrated on the interconnection of vehicle energy storage and grids [6]–[17]. Their goals are to educate others about the environmental and

Manuscript received September 16, 2010; revised December 15, 2010; accepted May 25, 2011. Date of publication September 1, 2011; date of current version February 23, 2012.

A. Y. Saber is with the Research and Development Department, ETAP, Irvine, CA 92618 USA (e-mail: aysaber@ieee.org).

G. K. Venayagamoorthy is with the Real-Time Power and Intelligent Systems Laboratory, Missouri University of Science and Technology, Rolla, MO 65409 USA (e-mail: gkumar@ieee.org).

Color versions of one or more of the figures in this paper are available online at <http://ieeexplore.ieee.org>.

Digital Object Identifier 10.1109/JSYST.2011.2163012

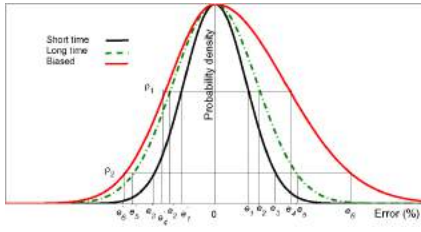


Fig. 1. Forecasted or estimated error distribution.

economic benefits of PHEVs and EVs, and to enhance the product market. However, PHEVs and EVs cannot completely solve the emission problem alone; they need electric power, which is one of the main sources of emissions. Therefore, the success of practical applications of PHEVs and EVs greatly depends on the maximum utilization of renewable energy in the smart grid so that emissions and costs are reduced. A smart grid in which there exists a sufficient power supply to meet customer needs with minimum cost and emissions should be adequate. PHEVs and EVs with additional vehicle-to-grid capabilities and RESs in a smart grid can help in this issue. RESs are cheap (considering operation costs); however, they have the problem of uncertainty. In unit commitment (UC), the forecasting load is used for scheduling, and the actual load usually differs from the forecasted one [18]. In this model, the number of vehicles is estimated to minimize cost and emissions; however, uncertainty surrounds the controllability of the vehicles for charging and discharging operations. Thus, unit commitment with plug-in vehicles under the uncertainties of wind and solar resources, load and vehicles are proposed in this paper for cost and emission reductions in smart grids. For optimization with uncertainty [19], a set of valid scenarios is considered in the UC with plug-in vehicles for the uncertainties of wind and solar energy, load and vehicles. A dynamic optimization is able to dynamically optimize the time varying resources such as RESs and GV in a complex smart grid.

The primary contributions of this paper are namely: 1) it considers the uncertainties of wind and solar energy, load, and vehicles in UC with plug-in vehicles; 2) it demonstrates the intelligent and flexible operation of gridable vehicles either as loads, sources, or energy storage units; 3) it illustrates the effectiveness of gridable vehicles in a smart grid with RESs under uncertainty; and 4) it bridges electricity and transportation infrastructures through the smart grid.

II. PROBLEM FORMULATION OF UC WITH PLUG-IN VEHICLES

Due to uncertainties in load demand, renewable sources (wind, solar) and the controllability of vehicles in smart grids, the planning of electricity production faces a major problem when determining the schedule of generating units and gridable vehicles. Therefore, decisions should be made in the presence of uncertainty for unit commitment with plug-in vehicles in smart grids. A probability distribution presenting the nature of uncertainty is either known with certainty or can be estimated from prior experiences on the system. Uncertainty

varies with time as well. A general uncertainty model of system variables such as wind and solar resources, load or vehicles can be represented in Fig. 1, where mean and standard deviation depend on the nature of the system variables. Some representative discrete states, called scenarios, are extracted for the optimization of UC with plug-in vehicles under uncertainty for simplicity, as it is difficult to consider all continuous states. However, the total number of scenarios grows exponentially with state variables (wind and solar resources, load and vehicles) and the total scheduling period.

The actual load differs from forecasted load. Researchers have analyzed the short-term load forecasting results for the past few years. The predicted percentage load demand deviation is usually from $\pm 1\%$ to $\pm 7\%$ [20], [21]. From prior statistics, the distribution may be biased (positively or negatively) or symmetric. In Fig. 1, positive error e_i may not be the same absolute value of negative error e_i with the same probability ρ_j . Similarly, due to the stochastic nature of wind and solar insolation, the output power from wind and solar farms cannot be predicted accurately. Uncertainty in GV controllability is also a problem. From prior statistics, a vehicle sits in a parking lot or at a home garage about 90%–95% time of a day. Therefore, uncertainty distribution of GVs is also considered in this model. General discrete probability distribution with error is shown in Fig. 1. For uncertainty, discrete probability distribution sets for load demand (δ_D), wind resources (δ_W), solar resources (δ_{PV}), and vehicles (δ_{V2G}) are given as follows:

$$\delta_D = \{(D^1, \rho_d^1); (D^2, \rho_d^2); \dots; (D^{nd}, \rho_d^{nd})\}$$

$$\rho_d^1 + \rho_d^2 + \dots + \rho_d^{nd} = 1$$

$$\delta_W = \{(P_{wind}^1, \rho_w^1); (P_{wind}^2, \rho_w^2); \dots; (P_{wind}^{nw}, \rho_w^{nw})\}$$

$$\rho_w^1 + \rho_w^2 + \dots + \rho_w^{nw} = 1$$

$$\delta_{PV} = \{(P_{solar}^1, \rho_{pv}^1); (P_{solar}^2, \rho_{pv}^2); \dots; (P_{solar}^{npv}, \rho_{pv}^{npv})\}$$

$$\rho_{pv}^1 + \rho_{pv}^2 + \dots + \rho_{pv}^{npv} = 1$$

$$\delta_{V2G} = \{(V2G^1, \rho_v^1); (V2G^2, \rho_v^2); \dots; (V2G^{nv}, \rho_v^{nv})\}$$

$$\rho_v^1 + \rho_v^2 + \dots + \rho_v^{nv} = 1$$

$$S = \delta_D \times \delta_W \times \delta_{PV} \times \delta_{V2G}$$

$$\sum_{s \in S} \rho_d \rho_w \rho_{so} \rho_v = 1.$$

Here, ρ is the corresponding probability of uncertain load demand, wind and solar resources or vehicles. A set of possible scenarios (S) is derived from the product of δ_D , δ_W , δ_{PV} , and δ_{V2G} .

Emissions are expressed as a polynomial function [22], and the order depends on the desired accuracy. In this paper, a quadratic function is considered for the emission curve as follows:

$$\mathcal{E}C_i(P_i(t)) = \alpha_i + \beta_i P_i(t) + \gamma_i (P_i(t))^2 \quad (1)$$

$$[\mathcal{E}C_i(P_i^s(t)), \rho_s] = [\alpha_i + \beta_i P_i^s(t) + \gamma_i (P_i^s(t))^2, \rho_s] \quad (2)$$

where α_i , β_i , and γ_i are emission coefficients of unit i , and $P_i(t)$ is the output level of unit i at time t . Equations (2) and (1) are for considering and not considering uncertainty, respectively. $P_i^s(t)$ and ρ_s are the output levels of unit i at time t considering scenario s and the probability of scenario s , respectively.

The fuel cost of a thermal unit is typically expressed as a second-order function of the unit's generated power

$$\mathcal{F}C_i(P_i(t)) = a_i + b_i P_i(t) + c_i (P_i(t))^2 \quad (3)$$

$$[\mathcal{F}C_i(P_i^s(t)), \rho_s] = [a_i + b_i P_i^s(t) + c_i (P_i^s(t))^2, \rho_s] \quad (4)$$

where a_i , b_i , and c_i are positive fuel cost coefficients of unit i . $P_i^s(t)$ and ρ_s are the same as above.

The start-up cost for restarting a decommitted thermal unit, which is related to the temperature of the boiler, is included in the model

$$\mathcal{S}C_i(t) = \begin{cases} h\text{-cost}_i, & \text{if boiler temperature} \geq \text{threshold} \\ c\text{-cost}_i, & \text{if boiler temperature} < \text{threshold}. \end{cases} \quad (5)$$

Gridable vehicles are considered as loads or sources. In a system considering GVs, the power supplied from distributed generations must satisfy the load demand and the system losses, which are defined as

$$\sum_{i=1}^N P_i^s(t) + P_{\text{solar}}^s(t) + P_{\text{wind}}^s(t) + \sum_{j=1}^{N_{\text{V2G}}^s(t)} \xi P_{v_j}(\Psi_{\text{pre}} - \Psi_{\text{dep}}) = D^s(t) + \text{Losses}, \quad \text{if GVs are sources} \quad (6)$$

$$\sum_{i=1}^N P_i^s(t) + P_{\text{solar}}^s(t) + P_{\text{wind}}^s(t) = D^s(t) + \sum_{j=1}^{N_{\text{V2G}}^s(t)} \xi P_{v_j}(\Psi_{\text{dep}} - \Psi_{\text{pre}}) + \text{Losses}, \quad \text{if GVs are loads.} \quad (7)$$

Only registered gridable vehicles are considered for smart operation, which they take part in during a predefined scheduling period

$$\sum_{t=1}^H N_{\text{V2G}}^s(t) = N_{\text{V2G}}^{\text{max}}. \quad (8)$$

To maintain system reliability, adequate spinning reserves are required:

$$\sum_{i=1}^N P_i^{\text{max}}(t) + P_{\text{solar}}^s(t) + P_{\text{wind}}^s(t) + \sum_{j=1}^{N_{\text{V2G}}^s(t)} P_{v_j}(\Psi_{\text{pre}} - \Psi_{\text{min}}) \geq D^s(t) + \text{Losses} + R(t) \quad (9)$$

if GVs are sources and

$$\sum_{i=1}^N P_i^{\text{max}}(t) + P_{\text{solar}}^s(t) + P_{\text{wind}}^s(t) \geq \sum_{j=1}^{N_{\text{V2G}}^s(t)} P_{v_j}(\Psi_{\text{dep}} - \Psi_{\text{pre}}) + D^s(t) + \text{Losses} + R(t) \quad (10)$$

if GVs are loads.

Each unit has a generation range, which is represented as

$$P_i^{\text{min}} \leq P_i^s(t) \leq P_i^{\text{max}}. \quad (11)$$

TABLE I
PLANT SIZE AND CAPACITY (1662 MW) OF 10-UNIT SYSTEM

	Unit 1	Unit 2	Unit 3	Unit 4	Unit 5
P_i^{max} (MW)	455	455	130	130	162
P_i^{min} (MW)	150	150	20	20	25
	Unit 6	Unit 7	Unit 8	Unit 9	Unit 10
P_i^{max} (MW)	80	85	55	55	55
P_i^{min} (MW)	20	25	10	10	10

Depletion of storage up to a certain minimum level and charging up to a maximum level are ensured to prevent loss of battery life, as represented below

$$\Psi_{\text{min}} P_{v_j} \leq P_{v_j}(t) \leq \Psi_{\text{max}} P_{v_j}. \quad (12)$$

Each vehicle has a desired departure state of charge level (Ψ), and charging/discharging inverter efficiencies are also considered in the model.

In the proposed model, emissions (2) and generation costs (4), (5) are considered as the objective of smart grids and the load balance (6), (7), registered vehicles (8), reliability reserve (9), (10), generation limit (11), state of charge, battery efficiency, parking lot limitations, and others are constraints.

Therefore, the objective (fitness) function for cost-emission optimization considering a set of scenarios S in a smart grid is

$$\min_{I_i(t), N_{\text{V2G}}(t)} \left\{ E \left(\sum_{s \in S} \sum_{i=1}^N \sum_{t=1}^H [\mathcal{W}_c (\mathcal{F}C_i(P_i^s(t)) + \mathcal{S}C_i(1 - I_i(t-1))) + \mathcal{W}_e (\psi_i \mathcal{E}C_i(P_i^s(t)))] I_i(t) \right) \right\} \quad (13)$$

or

$$\min_{I_i(t), N_{\text{V2G}}(t)} \left\{ \sum_{s \in S} \rho_w \rho_{\text{PV}} \rho_d \rho_v \sum_{i=1}^N \sum_{t=1}^H [\mathcal{W}_c (\mathcal{F}C_i(P_i^s(t)) + \mathcal{S}C_i(1 - I_i(t-1))) + \mathcal{W}_e (\psi_i \mathcal{E}C_i(P_i^s(t)))] I_i(t) \right\} \quad (14)$$

subject to (6)–(12) constraints. ψ_i is the emission penalty factor of unit i . Weight factors \mathcal{W}_c and \mathcal{W}_e are used to increase the system's flexibility.

III. COST AND EMISSION OPTIMIZATION

An intelligent optimization method is needed to handle uncertainty, large numbers of GVs and the proper utilization of RESs in smart grids to reduce cost and emissions. Particle swarm optimization (PSO) is used in this paper to minimize cost and emissions. PSO is similar to other swarm-based evolutionary algorithms [23]. Each potential solution, called a particle, flies in a multi-dimensional problem space with a velocity that is dynamically adjusted according to its flying experiences and its colleagues. PSO is an intelligent iterative method in which velocity and the position of each particle are calculated as follows:

$$v_{ij}(k) = [v_{ij}(k) + c_1 \text{rand}_1 (pbest_{ij}(k) - x_{ij}(k)) + c_2 \text{rand}_2 (gbest_j(k) - x_{ij}(k))] [1 + \frac{-\text{Range}}{\text{MaxIte}} (\text{Ite} - 1)]. \quad (15)$$

TABLE II
DISCRETE PROBABILITY DISTRIBUTION OF WIND AND SOLAR RESOURCES, LOAD AND VEHICLES

Prob.	Wind Expected (1 h–11 h)	Expected (12 h–24 h)	Prob.	Solar Expected (1 h–11 h)	Expected (12 h–24 h)	Prob.	Load Expected (1 h–11 h)	Expected (12 h–24 h)	Prob.	Vehicles Expected (1 h–11 h)	Expected (12 h–24 h)
0.50	100%	100%	0.70	100%	100%	0.60	100%	100%	0.60	100%	100%
0.15	99%	98%	0.15	98.5%	97.5%	0.15	98.5%	98%	0.20	98%	96%
0.15	101%	102%	0.15	101.5%	102.5%	0.15	102%	103%	0.20	103%	105%
0.10	97.5%	95%				0.05	98%	97%			
0.10	102.5%	105%				0.05	103%	104%			

Expected value $x\%$ means expected value is $x\%$ of the forecasted or estimated value, “Prob.” stands for probability.

TABLE III
SCHEDULE AND DISPATCH OF 10-UNIT SYSTEM (WITHOUT RENEWABLE SOURCES AND GVS)

Time (H)	U-1 (MW)	U-2 (MW)	U-3 (MW)	U-4 (MW)	U-5 (MW)	U-6 (MW)	U-7 (MW)	U-8 (MW)	U-9 (MW)	U-10 (MW)	V2G/G2V (MW)	Solar (MW)	Wind (MW)	Emission (ton)	Capacity (MW)	Demand* (MW)	Reserve (MW)
H 1	455.0	258.9	0.0	0.0	0.0	0.0	0.0	0.0	0.0	0.0	–	–	–	7175.83	910.0	700.0	210.0
H 2	455.0	180.0	0.0	130.0	0.0	0.0	0.0	0.0	0.0	0.0	–	–	–	6755.91	1040.0	750.0	290.0
H 3	455.0	152.0	130.0	130.0	0.0	0.0	0.0	0.0	0.0	0.0	–	–	–	7165.89	1170.0	850.0	320.0
H 4	455.0	253.9	130.0	130.0	0.0	0.0	0.0	0.0	0.0	0.0	–	–	–	8393.64	1170.0	950.0	220.0
H 5	455.0	280.0	130.0	130.0	25.0	0.0	0.0	0.0	0.0	0.0	–	–	–	8972.93	1332.0	1000.0	332.0
H 6	455.0	382.0	130.0	130.0	25.0	0.0	0.0	0.0	0.0	0.0	–	–	–	10681.11	1332.0	1100.0	232.0
H 7	455.0	433.0	130.0	130.0	25.0	0.0	0.0	0.0	0.0	0.0	–	–	–	11853.29	1332.0	1150.0	182.0
H 8	455.0	455.0	130.0	130.0	53.9	0.0	0.0	0.0	0.0	0.0	–	–	–	12378.27	1332.0	1200.0	132.0
H 9	455.0	455.0	130.0	130.0	110.9	20.0	25.0	0.0	0.0	0.0	–	–	–	13003.19	1497.0	1300.0	197.0
H10	455.0	455.0	130.0	130.0	162.0	60.9	25.0	10.0	0.0	0.0	–	–	–	13856.22	1552.0	1400.0	152.0
H11	455.0	455.0	130.0	130.0	162.0	80.0	25.0	31.9	10.0	0.0	–	–	–	14172.30	1607.0	1450.0	157.0
H12	455.0	455.0	130.0	130.0	162.0	80.0	25.0	55.0	27.9	10.0	–	–	–	14122.31	1662.0	1500.0	162.0
H13	455.0	455.0	130.0	130.0	162.0	80.0	25.0	17.5	0.0	0.0	–	–	–	13541.61	1552.0	1400.0	152.0
H14	455.0	455.0	130.0	130.0	136.9	20.0	25.0	0.0	0.0	0.0	–	–	–	13125.73	1497.0	1300.0	197.0
H15	455.0	455.0	130.0	130.0	77.9	0.0	0.0	0.0	0.0	0.0	–	–	–	12395.62	1332.0	1200.0	132.0
H16	455.0	351.9	130.0	130.0	25.0	0.0	0.0	0.0	0.0	0.0	–	–	–	10067.43	1332.0	1050.0	282.0
H17	455.0	300.0	130.0	130.0	25.0	0.0	0.0	0.0	0.0	0.0	–	–	–	9137.12	1332.0	1000.0	332.0
H18	455.0	404.0	130.0	130.0	25.0	0.0	0.0	0.0	0.0	0.0	–	–	–	11166.84	1332.0	1100.0	232.0
H19	455.0	455.0	130.0	130.0	32.9	20.0	25.0	0.0	0.0	0.0	–	–	–	12914.61	1497.0	1200.0	297.0
H20	455.0	455.0	130.0	130.0	162.0	80.0	25.0	17.5	0.0	0.0	–	–	–	13541.61	1552.0	1400.0	152.0
H21	455.0	455.0	130.0	130.0	136.9	20.0	25.0	0.0	0.0	0.0	–	–	–	13125.73	1497.0	1300.0	197.0
H22	455.0	404.0	130.0	130.0	25.0	0.0	0.0	0.0	0.0	0.0	–	–	–	11166.84	1332.0	1100.0	232.0
H23	455.0	221.0	130.0	130.0	0.0	0.0	0.0	0.0	0.0	0.0	–	–	–	7800.11	1170.0	900.0	270.0
H24	455.0	247.0	0.0	130.0	0.0	0.0	0.0	0.0	0.0	0.0	–	–	–	7484.43	1040.0	800.0	240.0

Considering uncertainty, expected running cost = \$568825.84 (fuel cost plus start-up cost) and expected emission = 255774.81 tons
Number of scenarios = 5, execution time = 82.94 s.

Demand* is forecasted and five scenarios are considered for the uncertainty of the load demand.

Binary PSO for generating units

$$I_{ij}(k+1) = x_{ij}(k+1) = \begin{cases} 1, & \text{if } U(1) < \frac{1}{1+\exp(-v_{ij}(k))} \\ 0, & \text{otherwise.} \end{cases} \quad (16)$$

Integer PSO for GVs

$$N_{V2G_j}(k+1) = x_{ij}(k+1) = \text{round}(x_{ij}(k) + v_{ij}(k)). \quad (17)$$

Here, I_{ij} and x_{ij} are matrices of sizes $(H \times N)$ and $(H \times N + 1)$, respectively. However, N_{V2G_j} is a column vector of $(H \times 1)$ integers that reduces dimensions; and it is assigned to the last column of matrix x_{ij} . $pbest$, $gbest$, v , x , w , c_1 , and c_2 are standard terms, and (15)–(17) are standard equations of PSO [23].

The flowchart in Fig. 2 shows that PSO minimizes cost and emissions in a smart grid integrated with GVs and RESs considering the uncertainties of wind and solar, load and vehicles. In the proposed solution model, binary PSO optimizes the on/off states of power generating units. GVs are represented by integer numbers instead of zeros and ones to reduce the dimension of the problem. Integer PSO optimizes the number of GVs in the constrained system, provides balance between local and global searching abilities, and finds balance

between cost and emission reductions. At hour t , if the schedule is $[I_1(t), I_2(t), \dots, I_N(t), N_{V2G}(t), P_{pv}(t), P_{wind}(t)]^T$, then for all the scenarios $s \in \mathcal{S}$, the power to and from the vehicles is $\xi N_{V2G}^s(t) P_{vi}(\Psi_{pre} - \Psi_{dep})$; sign of $N_{V2G}(t)$ indicates load/source; and the remaining demand $[D^s(t) + \xi N_{V2G}^s(t) P_{vi}(\Psi_{pre} - \Psi_{dep}) - P_{pv}^s(t) - P_{wind}^s(t)]$ is fulfilled (dispatched) from conventional running units of the schedule $[I_1(t), I_2(t), \dots, I_N(t)]^T$ using Lambda iteration. $D^s(t)$, $N_{V2G}^s(t)$, $P_{pv}^s(t)$, and $P_{wind}^s(t)$ are calculated using scenario s with known discrete certainty. For example, if a scenario s has $xd\%$ more load with probability ρ_d , $xw\%$ more wind power with probability ρ_w , $xpv\%$ less solar power with probability ρ_{pv} and $xv\%$ more vehicles with probability ρ_v , then $D^s(t) = (1 + xd)D(t)$, $P_{wind}^s(t) = (1 + xw)P_{wind}(t)$, $P_{pv}^s(t) = (1 - xpv)P_{pv}(t)$, $N_{V2G}^s(t) = (1 + xv)N_{V2G}(t)$, and their joint probability is $\rho_d \rho_w \rho_{pv} \rho_v$.

IV. RESULTS AND DISCUSSIONS

An independent system operator (ISO) of a 10-unit system is considered for simulation with 50 000 GVs. Load demand and unit characteristics of the 10-unit system are

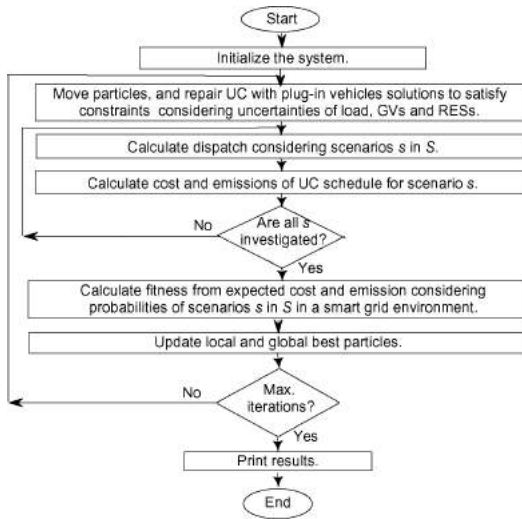


Fig. 2. Flowchart of UC with plug-in vehicles considering uncertainty in a smart grid environment.

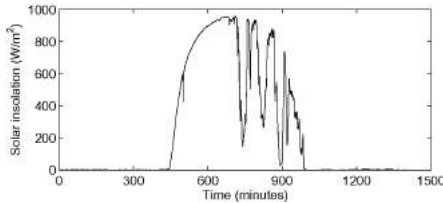


Fig. 3. Average solar insolation in a random day used for analysis in this paper.

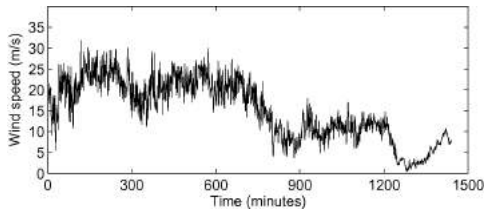


Fig. 4. Average wind speed in a random day used for analysis in this paper.

collected from [24], and emission coefficients are collected from [25]. Plant size is shown in Table I. Discrete probability distribution of wind and solar resources, load and vehicles are shown in Table II. The distributions of wind and solar resources are symmetric; however, they are positively biased for load and vehicles. Actually, the uncertainty distribution depends on location, the nature of state variables and the forecasting/estimation tools that are used. In Table II, the expected value $x\%$ means that the expected value is $x\%$ of the forecasted or estimated value. The authors establish the discrete probabilities and expected values in the table from their prior experience.

The parameter values used in this paper are the same as in [25]. For practical applications, the number of GV's in an electric power network can be estimated analytically based on the number of electricity clients (customers) in that network. In the 10-unit ISO, a reasonable number of GV's is 50 000 [25].

A linear approximate model is applied to estimate vehicle emissions. An average distance driven by a vehicle is about

12 000 miles per year [25]. Average emission from light weight vehicles is 1.2 lbs/mile. Thus, emissions from a light weight vehicle over a year are $(12\,000 \times 1.2 =) 144\,000$ lbs, and the total emissions from 50 000 mechanical vehicles are 7 200 000 000 lbs (3266787.66 tons).

Cost and emissions are calculated for the 10-unit system with standard input data of power plants, emission coefficients and load demand without considering GV's and RESs. PSO is used to calculate the schedule, power dispatch and corresponding emissions. Uncertainty only comes from the forecasted load. Five scenarios are considered for the load uncertainty. Results are shown in Table III. Expected running cost and emission are \$568825.84 and 255774.81 tons, respectively. Execution time is 82.94 s.

A smart grid consists of RESs, GV's, and thermal units in which GV's can be used as loads, sources, and storage units. For a small city of 50 000 GV's, each day at least $(50\,000 \times 15\text{ kWh} =) 750$ MWh of wind and solar power is needed to achieve the full benefit of the GV's for reducing cost and emissions. If the power generation ratio from wind and solar sources is 2:1, 500 MWh of power comes from wind and 250 MWh from the sun. This assumption is based on the good wind speed and solar insolation profiles for the location studied. In this paper, solar insolation data are collected from NREL's Solar Radiation Research Laboratory [26], Golden, CO, for the solar farm model in the smart grid. Wind speed data are collected from the National Wind Technology Center [27], Boulder, CO, for the wind farm model in the smart grid. Figs. 3 and 4 are used to estimate realistic wind farm and solar farm sizes. However, for a given location, this can be formulated and solved using an optimization algorithm to find a near-optimal size based on wind speed and solar insolation data over a period of time

$$A\beta[\mu(t=1) + \mu(t=2) + \dots + \mu(t=24)] = 250\text{ MW}. \quad (18)$$

Using the above equation and 16% efficiency (β), the maximum capacity of the solar farm is ≈ 40 MW for the small system. Similarly, the wind farm's size is calculated from the General Electric 1.5 sle 1.5 MW turbine data sheet [28]. Then, the forecasted wind and solar power are used in the simulation.

Results from a smart grid model with wind, solar and GV's under uncertainty are shown in Table IV, where GV's are operated as loads as well as sources. Uncertainties of wind and solar resources, load and GV's are considered here, and the total number of scenarios is huge, as it grows exponentially. Two-hundred twenty-five scenarios are considered in the simulation. Solar energy is available only during the daytime from 7 am to 4 pm, while wind energy is available most of the time. According to Table IV, GV's are charged from the grid at off-peak load during the 1st–7th, 16th–18th, and 22nd–24th hours. On the other hand, GV's are discharged to the grid at peak load during the 8th–15th and 19th–21st hours. So, GV's are operated as loads and storage units mainly at night from 10 pm to 7 am, as sources during working hours from 8 am to 3pm, and as loads or sources, depending on the system demand, the remainder of the time from 4 pm to 9 pm. According to the results, a significant amount of power is discharged to the grid as V2G at peak hours (11th and 12th

TABLE IV
SCHEDULE AND DISPATCH OF GENERATING UNITS, RESS AND GVS AS LOADS AS WELL AS SOURCES IN SMART GRID

Time (H)	U-1 (MW)	U-2 (MW)	U-3 (MW)	U-4 (MW)	U-5 (MW)	U-6 (MW)	U-7 (MW)	U-8 (MW)	U-9 (MW)	U-10 (MW)	V2G/G2V* (MW)	Solar* (MW)	Wind* (MW)	Emission (ton)	Capacity (MW)	Demand* (MW)	Reserve (MW)
H 1	455.0	155.9	0.0	130.0	0.0	0.0	0.0	0.0	0.0	0.0	-37.73	0.00	10.54	7409.87	1059.1	700.0	359.1
H 2	455.0	197.4	0.0	130.0	0.0	0.0	0.0	0.0	0.0	0.0	-40.26	0.00	22.27	8090.28	1060.3	750.0	310.3
H 3	455.0	168.1	130.0	130.0	0.0	0.0	0.0	0.0	0.0	0.0	-42.30	0.00	25.50	8232.95	1191.3	850.0	341.3
H 4	455.0	257.1	130.0	130.0	0.0	0.0	0.0	0.0	0.0	0.0	-29.29	0.00	25.50	8570.00	1184.9	950.0	234.9
H 5	455.0	310.6	130.0	130.0	25.0	0.0	0.0	0.0	0.0	0.0	-56.83	0.00	25.50	9319.62	1360.5	1000.0	360.5
H 6	455.0	397.9	130.0	130.0	25.0	0.0	0.0	0.0	0.0	0.0	-42.12	0.00	25.50	11041.54	1353.2	1100.0	253.2
H 7	455.0	455.0	130.0	130.0	50.9	0.0	0.0	0.0	0.0	0.0	-74.21	0.09	25.50	12379.56	1369.1	1150.0	219.1
H 8	455.0	383.6	130.0	130.0	25.0	0.0	0.0	0.0	0.0	0.0	56.50	17.46	25.50	10846.83	1360.4	1200.0	160.4
H 9	455.0	426.8	130.0	130.0	25.0	20.0	25.0	0.0	0.0	0.0	56.23	31.45	25.50	12544.66	1525.2	1300.0	225.2
H10	455.0	455.0	130.0	130.0	95.2	20.0	25.0	10.0	0.0	0.0	45.01	36.01	25.50	13275.78	1574.7	1400.0	174.7
H11	455.0	455.0	130.0	130.0	106.1	20.0	25.0	10.0	10.0	0.0	73.10	38.06	25.50	13617.52	1643.6	1450.0	193.6
H12	455.0	455.0	130.0	130.0	158.4	20.0	25.0	10.0	10.0	10.0	63.89	35.93	25.50	13834.44	1694.0	1500.0	194.0
H13	455.0	455.0	130.0	130.0	149.1	20.0	25.0	10.0	0.0	0.0	17.74	36.78	25.50	13529.76	1562.1	1400.0	162.1
H14	455.0	455.0	130.0	130.0	45.2	20.0	25.0	0.0	0.0	0.0	33.63	31.59	24.82	12897.71	1515.9	1300.0	215.9
H15	455.0	425.6	130.0	130.0	25.0	0.0	0.0	0.0	0.0	0.0	50.76	9.70	20.74	11874.19	1360.3	1200.0	160.3
H16	455.0	366.2	130.0	130.0	25.0	0.0	0.0	0.0	0.0	0.0	-42.69	12.92	14.62	10347.68	1355.8	1050.0	305.8
H17	455.0	292.0	130.0	130.0	25.0	0.0	0.0	0.0	0.0	0.0	-18.84	0.00	25.50	9030.88	1342.8	1000.0	342.8
H18	455.0	430.3	130.0	130.0	25.0	0.0	0.0	0.0	0.0	0.0	-46.35	0.00	19.04	11766.42	1357.9	1100.0	257.9
H19	455.0	394.5	130.0	130.0	25.0	20.0	25.0	0.0	0.0	0.0	41.74	0.00	25.50	11655.95	1520.4	1200.0	320.4
H20	455.0	455.0	130.0	130.0	138.1	20.0	25.0	10.0	0.0	0.0	73.89	0.00	18.02	13556.37	1593.0	1400.0	193.0
H21	455.0	455.0	130.0	130.0	25.0	20.0	25.0	0.0	0.0	0.0	88.60	0.00	25.50	12921.20	1546.1	1300.0	246.1
H22	455.0	410.0	130.0	130.0	25.0	0.0	0.0	0.0	0.0	0.0	-28.58	0.00	21.42	11836.97	1348.1	1100.0	248.1
H23	455.0	271.7	130.0	130.0	0.0	0.0	0.0	0.0	0.0	0.0	-50.76	0.00	0.00	8407.93	1198.3	900.0	298.3
H24	455.0	207.0	130.0	130.0	0.0	0.0	0.0	0.0	0.0	0.0	-92.74	0.00	2.55	8885.11	1221.4	800.0	421.4

Solar farm size = 40 MW (250731.33 m²)
Wind farm size = 25.5 MW (17 wind turbines and 1.5 MW each)
Considering uncertainty, expected running cost = \$554385.64 (fuel cost plus start-up cost) and expected emission = 249271.26 tons
Number of scenarios = 225, execution time = 1275.44 s.

Solar*, Wind*, and Demand* are forecasted, V2G/G2V* is estimated in PSO, positive and negative values of V2G/G2V indicate discharging and charging, respectively.

hours). However, the amount of power for V2G and G2V is not linearly proportional to the demand, as cost and emission are nonlinear functions of power output, and PSO optimizes both cost and emission here.

In Table IV, the expected running cost and emissions are \$554385.64 and 249271.26 tons, respectively, when 50 000 GVs are considered in the 10-unit system during 24 h in the smart grid. On the other hand, the expected running cost and emissions are \$568825.84 and 255774.81 tons, respectively, when RESS and GVs are not integrated in the same system (Table III). Thus, (255774.81 tons – 249271.26 tons=) 6503.55 tons of emissions per day or 2373795.75 tons per year is reduced from only power plants of the 10-unit small system in the smart grid. Besides 50 000 GVs will replace 50 000 conventional vehicles, and it is already calculated that emissions are 3266787.66 tons from the 50 000 light weight vehicles. So 50 000 GVs will eliminate 5640583.41 tons (2373795.75 tons + 3266787.66 tons) of emissions from power systems and the transportation sector.

Fuel costs are highly volatile. The benchmark fuel cost coefficients used in this simulation are old. Present cost coefficients are much higher, as current fuel costs have increased greatly in the last decade. According to the results, GVs save at least (\$568825.84 – \$554385.64=) \$14440.2 per day for the 10-unit small system. It will also save running costs from the transportation sector. It is assumed that the mileage of a light weight vehicle is 20 miles/gallon, the average tour length is 32.88 miles/day [25], and the present gasoline price is around \$2.5/gallon. Therefore, transportation costs will be reduced by

[50 000*(32.88 miles/20 miles)*\$2.5=] \$205 500 per day for the 50 000 GVs. Thus, the smart grid with RESSs and GVs can save at least (\$14440.2 + \$205 500=) \$219940.2 from the power system and transportation sectors every day. However, the system requires capital costs for the RESSs.

The execution time depends on the size of the system, the scheduling period, and the number of scenarios. It is an exponential function of the problem dimension and a polynomial function of the number of scenarios. To reduce the dimension of the problem, an individual vehicle is not scheduled (an aggregation of vehicles is scheduled). The total number of scenarios is huge; thus, only some selected desired scenarios are considered from prior experiences (or scenario reduction methods can be applied). The execution time is 82.94 s (Table III) when there are only five scenarios and no GVs or RESSs in the system. On the other hand, the execution time is 1275.44 s (Table IV) when the number of scenarios is 225 and GVs and RESSs are in the smart grid model. It is tolerable for offline calculations.

V. CONCLUSION

Unit commitment with plug-in vehicles under uncertainty has been presented in this paper to illustrate cost and emission reductions for a sustainable integrated electricity and transportation infrastructure. Particle swarm optimization has been used to generate a successful schedule considering the uncertainties of wind and solar energy, load and GVs in a smart grid. Valid scenarios are derived from prior statistics, heuristics and

the experiences of the authors. In UC with plug-in vehicles, GV's schedules are estimated with these uncertainties using the optimization method. This optimization with uncertainties for UC scheduling requires longer execution time; however, it is more reliable in real, dynamic environments. Furthermore, real-time prices and intelligent scenarios must be considered in the UC with plug-in vehicles in a smart grid environment.

REFERENCES

- [1] U. K. Madawala, P. Schweizer, and V. V. Haerri, "Living and mobility: A novel multipurpose in-house grid interface with plug-in hybrid BlueAngle," in *Proc. IEEE ICSET*, Nov. 2008, pp. 531–536.
- [2] S. Labatt and R. R. White, *Carbon Finance: The Financial Implications of Climate Change*. Hoboken, NJ: Wiley, 2007.
- [3] N. Stern. (2006). *The Stern Review: The Economics of Climate Change* [Online]. Available: <http://www.sternreview.org.uk>
- [4] K. Parks, P. Denholm, and T. Markel, "Costs and emissions associated with plug-in hybrid electric vehicle charging in the Xcel Energy Colorado service territory," Natl. Renewable Energy Lab., Golden, CO, Tech. Rep. NREL/TP-640-41410, May 2007.
- [5] Electric Power Research Institute, "Comparing the benefits and impacts of hybrid electric vehicle options for compact sedan and sport utility vehicles," EPRI, Palo Alto, CA, Tech. Rep. 1006891, Jul. 2002.
- [6] W. Kempton and J. Tomic, "Vehicle-to-grid power implementation: From stabilizing the grid to supporting large-scale renewable energy," *J. Power Sources*, vol. 144, no. 1, pp. 280–294, Jun. 2005.
- [7] J. Moreno, M. E. Ortúzar, and J. W. Dixon, "Energy-management system for a hybrid electric vehicle, using ultracapacitors and neural networks," *IEEE Trans. Ind. Electron.*, vol. 53, no. 2, pp. 614–623, Apr. 2006.
- [8] A. Emadi, Y. J. Lee, and K. Rajashekara, "Power electronics and motor drives in electric, hybrid electric, and plug-in hybrid electric vehicles," *IEEE Trans. Ind. Electron.*, vol. 55, no. 6, pp. 2237–2245, Jun. 2008.
- [9] A. Affanni, A. Bellini, G. Franceschini, P. Guglielmi, and C. Tassoni, "Battery choice and management for new-generation electric vehicles," *IEEE Trans. Ind. Electron.*, vol. 52, no. 5, pp. 1343–1349, Oct. 2005.
- [10] W. Kempton, J. Tomic, S. Letendre, A. Brooks, and T. Lipman, "Vehicle-to-grid power: Battery, hybrid and fuel cell vehicles as resources for distributed electric power in California," Instit. Transportation Stud., Davis, CA, Rep. IUCD-ITS-RR 01-03, Jun. 2001.
- [11] H.-S. Park, C.-E. Kim, C.-H. Kim, G. -W. Moon, and J.-H. Lee, "A modularized charge equalizer for an HEV lithium-ion battery string," *IEEE Trans. Ind. Electron.*, vol. 56, no. 5, pp. 1464–1476, May 2009.
- [12] J. Tomic and W. Kempton, "Using fleets of electric-drive vehicles for grid support," *J. Power Sources*, vol. 168, no. 2, pp. 459–468, Jun. 2007.
- [13] S. M. Lukic, J. Cao, R. C. Bansal, R. Rodriguez, and A. Emadi, "Energy storage systems for automotive applications," *IEEE Trans. Ind. Electron.*, vol. 55, no. 6, pp. 2258–2267, Jun. 2008.
- [14] W. Kempton and J. Tomic, "Vehicle to grid fundamentals: Calculating capacity and net revenue," *J. Power Sources*, vol. 144, no. 1, pp. 268–279, Jun. 2005.
- [15] B. D. Williams and K. S. Kurani, "Estimating the early household market for light-duty hydrogen-fuel-cell vehicles and other 'mobile energy' innovations in California: A constraints analysis," *J. Power Sources*, vol. 160, no. 1, pp. 446–453, Sep. 2006.
- [16] B. D. Williams and K. S. Kurani, "Commercializing light-duty plug-in/plug-out hydrogen-fuel-cell vehicles: 'Mobile electricity' technologies and opportunities," *J. Power Sources*, vol. 166, no. 2, pp. 549–566, Apr. 2007.
- [17] W. Kempton and T. Kubo, "Electric-drive vehicles for peak power in Japan," *Energy Policy*, vol. 28, no. 1, pp. 9–18, 2000.
- [18] A. Y. Saber, T. Senjyu, T. Miyagi, N. Urasaki, and T. Funabashi, "Fuzzy unit commitment scheduling using absolutely stochastic simulated annealing," *IEEE Trans. Power Syst.*, vol. 21, no. 2, pp. 955–964, May 2006.
- [19] N. Sahinidis, "Optimization under uncertainty: State-of-the-art and opportunities," *Comput. Chem. Eng.*, vol. 28, nos. 6–7, pp. 971–983, Jun. 2004.
- [20] A. H. Mantawy, "A genetic algorithm solution to a new fuzzy unit commitment model," *Electr. Power Syst. Res.*, vol. 72, no. 2, pp. 171–178, Dec. 2004.
- [21] C.-C. Su and Y.-Y. Hsu, "Fuzzy dynamic programming: An application to unit commitment," *IEEE Trans. Power Syst.*, vol. 6, no. 3, pp. 1231–1237, Aug. 1991.
- [22] P. Venkatesh, R. Gnanadass, and N. P. Padhy, "Comparison and application of evolutionary programming techniques to combined economic emission dispatch with line flow constraints," *IEEE Trans. Power Syst.*, vol. 18, no. 2, pp. 688–697, May 2003.
- [23] Y. Valle, G. K. Venayagamoorthy, S. Mohagheghi, J.-C. Hernandez, and R. G. Harley, "Particle swarm optimization: Basic concepts, variants and applications in power systems," *IEEE Trans. Evol. Comput.*, vol. 12, no. 2, pp. 171–195, Apr. 2008.
- [24] T. O. Ting, M. V. C. Rao, and C. K. Loo, "A novel approach for unit commitment problem via an effective hybrid particle swarm optimization," *IEEE Trans. Power Syst.*, vol. 21, no. 1, pp. 411–418, Feb. 2006.
- [25] A. Y. Saber and G. K. Venayagamoorthy, "Intelligent unit commitment with vehicle-to-grid: A cost-emission optimization," *J. Power Sources*, vol. 195, no. 3, pp. 898–911, Feb. 2010.
- [26] National Renewable Energy Laboratory (NREL), Solar Radiation Research Laboratory (SRRL), Golden, CO [Online]. Available: http://www.nrel.gov/midc/srrl_bms
- [27] National Renewable Energy Laboratory (NREL), National Wind Technology Center (NWTTC), Boulder, CO [Online]. Available: http://www.nrel.gov/midc/nwtc_m2
- [28] *General Electric 1.5 sle Datasheet* [Online]. Available: http://www.ge-energy.com/content/multimedia/_files/downloads/GEA18768_Wind_1.5-77_Broch_r7.pdf



Ahmed Yousuf Saber (S'04–M'07–SM'10) received the B.Sc. and M.Sc. degrees from the Bangladesh University of Engineering and Technology, Dhaka, Bangladesh, and the Ph.D. degree from the University of the Ryukyus, Okinawa, Japan.

He served as an Assistant Professor with the University of Asia Pacific, Dhaka, and King Abdulaziz University, Jeddah, Saudi Arabia. He was a Visiting Scholar with the Missouri University of Science and Technology, Rolla. He is currently with the Research and Development Department, ETAP, Irvine, CA.

His current research interests include smart-grid, vehicle-to-grid, renewable energy, cyber-physical systems, state and load estimation of unbalanced distribution systems, and operation research.



Ganesh Kumar Venayagamoorthy (S'91–M'97–SM'02) received the Ph.D. degree in electrical engineering from the University of Natal, Durban, South Africa, in 2002.

He is currently a Professor of Electrical and Computer Engineering, and the Founder and Director of the Real-Time Power and Intelligent Systems Laboratory, Missouri University of Science and Technology, Rolla. He has published over 390 refereed articles. His current research interests include the development and applications of emerging computational algorithms for power systems stability and control, and smart grid applications.

Dr. Venayagamoorthy is a recipient of several awards, and has been involved in the leadership and organization of many conferences.